ARTICLE

KLF4 initiates sustained YAP activation to promote renal fibrosis in mice after ischemia-reperfusion kidney injury

Dan Xu[1], Pan-pan Chen[1], Pei-qing Zheng[1], Fan Yin[1], Qian Cheng[1], Zhuan-li Zhou[1], Hong-yan Xie[1], Jing-yao Li[1], Jia-yun Ni[1], Yan-zhe Wang[2], Si-jia Chen[2], Li Zhou[1], Xiao-xia Wang[2], Jun Liu[1], Wei Zhang[1] and Li-min Lu[1]

Acute renal injury (AKI) causes a long-term risk for progressing into chronic kidney disease (CKD) and interstitial fibrosis. Yes-associated protein (YAP), a key transcriptional cofactor in Hippo signaling pathway, shuttles between the cytoplasm and nucleus, which is required for the renal tubular epithelial cells repair in the acute phase of AKI. In this study we investigated the role of YAP during ischemia-reperfusion (IR)-induced AKI to CKD. Mice were subjected to left kidney IR followed by removal of the right kidney on the day before tissue harvests. Mouse shRNA expression adenovirus (Ad-shYAP or Ad-shKLF4) and mouse KLF4 expression adenovirus (Ad-KLF4) were delivered to mice by intrarenal injection on D7 after IR. We showed that the expression and nucleus distribution of YAP were persistently increased until the end of experiment (D21 after IR). The sustained activation of YAP in post-acute phase of AKI was accompanied by renal dysfunction and interstitial fibrosis. Knockdown of YAP significantly attenuated IR-induced renal dysfunction and decreased the expression of fibrogenic factors TGF-β and CTGF in the kidney. We showed that the expression of the transcription factor KLF4, lined on the upstream of YAP, was also persistently increased. Knockdown on KLF4 attenuated YAP increase and nuclear translocation as well as renal functional deterioration and interstitial fibrosis in IR mice, whereas KLF4 overexpression caused opposite effects. KLF4 increased the expression of ITCH, and ITCH facilitated YAP nuclear translocation via degrading LATS1. Furthermore, we demonstrated in primary cultured renal tubular cells that KLF4 bound to the promoter region of YAP and positively regulates YAP expression. In biopsy sample from CKD patients, we also observed increased expression and nuclear distribution of YAP. In conclusion, the activation of YAP in the post-acute phase of AKI is implicated in renal functional deterioration and fibrosis although it exhibits beneficial effect in acute phase. Reprogramming factor KLF4 is responsible for the persistent activation of YAP. Blocking the activation of KLF4-YAP pathway might be a way to prevent the transition of AKI into CKD.

Keywords: ischemia-reperfusion kidney injury; chronic kidney disease; YAP; KLF4; ITCH; renal tubular epithelial cells

INTRODUCTION

Acute kidney injury (AKI) is an important clinical condition associated with high morbidity and mortality [1, 2]. Approximately 28.5% of AKI patients do not recover completely with the disease progressing into chronic kidney disease (CKD), and 8.6% of these patients ultimately experienced end-stage renal disease [3, 4].

Ischemia-reperfusion (IR) is a common cause of AKI in the clinic [5]. The prognosis of IR-induced renal injury largely depends on the degree of ischemia and the manner of reperfusion. Renal function usually recovers in a week after mild IR. Severe damage following prolonged IR can cause maladaptive repair, manifested as irreversible renal damage and even fibrotic scar formation [6, 7]. Although an increasing amount of research has focused on this process in recent decades, the mechanism of post-AKI renal injury is still not fully understood.

Renal tubules, especially proximal tubules, are the major targets of IR-induced renal injury [8, 9]. After IR induction, some renal tubular epithelial cells are necrotic and detach from the basal membrane. Residual tubular epithelial cells undergo a dedifferentiation transition and acquire the ability of proliferation to repair damaged tubules [10, 11]. Maladaptive repair in renal tubules has also been found to be a driving force for the progression of AKI to CKD [12–14].

The Hippo signaling pathway is highly conserved in mammals [15]. It has been implicated in organ and tissue growth because it regulates cell differentiation, proliferation, and apoptosis [16–18]. Yes-associated protein (YAP), the key transcriptional cofactor in the Hippo signaling pathway [19], shuttles between the cytoplasm and nucleus [20, 21]. Phosphorylated YAP (P-YAP) stays in the cytoplasm, while dephosphorylated YAP is translocated into the nucleus where it interacts with TEA domain family member to stimulate the expression of downstream genes, including profibrotic genes such as transforming growth factor-β (TGF-β) [22] and connective tissue growth factor (CTGF) [23, 24].

Large tumor suppressor 1 (LATS1), a serine/threonine kinase, is the key enzyme for the YAP phosphorylation modification that

[1]Department of Physiology and Pathophysiology, School of Basic Medical Sciences, Shanghai Medical College, Fudan University, Shanghai 200032, China and [2]Department of Nephrology, Shanghai Tong Ren Hospital, Shanghai Jiao Tong University School of Medicine, Shanghai 200032, China
Correspondence: Wei Zhang (wzhang@shmu.edu.cn) or Li-min Lu (lulimin@shmu.edu.cn)
These authors contributed equally: Dan Xu, Pan-pan Chen

Sustained activation of KLF4-YAP promotes renal fibrosis
D Xu et al.

437

restricts YAP to the cytoplasm [25, 26]. In contrast, Itchy E3 ubiquitin protein ligase (ITCH) promotes YAP nuclear translocation by facilitating LATS1 polyubiquitination-directed degradation [27]. It has been reported that YAP activation is required for renal tubular epithelial cell repair in the acute phase of AKI. Knocking out YAP delayed renal function and structure recovery after IR injury [23].

The transcription factor KLF4 is a member of the zinc finger family [28]. It is known as one of four factors that reprogram terminally differentiated cells into pluripotent stem cells. KLF4 is a dual-function transcription factor that can activate or inhibit the transcription of genes regulating cell proliferation, differentiation, apoptosis, and cell reprogramming [29–33].

In IR-induced renal fibrotic mice, our preliminary data showed that YAP was elevated and activated after the acute phase of AKI. In the related experiment, the role of the sustained activation of YAP was investigated in IR-induced AKI to CKD animal model. Our results demonstrated that the sustained activation of YAP in the post-acute phase was associated with renal function decline and fibrosis. The activation of YAP stimulated the production of the profibrotic factors TGF-β and CTGF in renal tubular epithelial cells and then promoted the activation of interstitial fibroblasts. The reprogramming factor KLF4 was involved in the sustained activation of YAP by upregulating YAP expression as well as nuclear translocation.

MATERIALS AND METHODS

Animals and surgical procedures
Eight-week-old male C57BL/6J mice (25–30 g) were purchased from Shanghai SLAC Laboratory Animal Co. (Shanghai, China). All animal experiments were performed according to the criteria of the Medical Laboratory Animal Administrative Committee of Shanghai and the Guide for Care and Use of Laboratory Animals of Fudan University, and the protocols were approved by the Ethics Committee for Experimental Research, Shanghai Medical College, Fudan University. The mice were subjected to unilateral renal IR by an established protocol described previously [34, 35]. In brief, the left renal pedicle was clamped for 45 min followed by removal of the clamp to allow reperfusion of the kidney. The day before tissue harvesting, the intact right kidney was removed through a right flank incision. To study the effect of YAP and KLF4, three sets of experiments were performed. Briefly, mouse YAP or KLF4 siRNA was ligated into a plasmid and then recombined into an adenovirus vector (Ad-shRNA). Mouse shRNA expression adenovirus (Ad-shYAP or Ad-shKLF4) or mouse KLF4 expression adenovirus (Ad-KLF4), obtained from Hanbio Biotechnology (Shanghai, China), was delivered into mouse kidneys as described previously [36].

Evaluation of renal function
Urine albumin and urine creatinine were assessed using the QuantiChrom creatinine assay kit (DICT-500, BioAssay Systems, CA, USA) and BCG albumin assay kits (DIAG-250, BioAssay Systems, CA, USA). Urinary albumin to creatinine ratio (ACR, gram per gram) was calculated as follows: urine albumin (gram per liter)/urine creatinine (gram per liter). The Scr level was measured by an automatic chemistry analyzer (Cobas C 501, Roche, Basel, Switzerland).

Histological examination
The tubular injury score was estimated in renal tissue stained with hematoxylin and eosin. The percentage of damaged tubules was calculated on the basis of renal tubule dilation, hyaline cast formation, epithelial cell atrophy, and interstitial inflammatory cell infiltration. Six high-power fields (original magnification of ×400)

were chosen randomly. The mean values of the percentage as determined by three investigators were reported.

Masson's trichrome staining was used to detect renal fibrosis as determined by routine procedures in mouse kidneys and renal biopsy specimens from patients with CKD. The renal fibrotic area indicated by blue staining was scored. The percentage of fibrotic area in each image was counted by an investigator blinded to the experimental conditions.

Immunohistochemistry
Paraffin-embedded mouse kidney sections were used to conduct immunohistochemistry (IHC) in a routine procedure. The antibodies used in the study were anti-KLF4 (ab106629, Abcam, Cambridge, MA, USA), anti-YAP (14074T, Cell Signaling Technology, Danvers, MA, USA), anti-fibronectin (15613-1-AP, Proteintech, Chicago, IL, USA), anti-α-SMA (14395-1-AP, Proteintech, Chicago, IL, USA), and anti-LATS1 (17049-1-AP, Proteintech, Chicago, IL, USA). Ten randomly selected high-power fields (original magnification ×400) per section were quantified by an investigator blinded to the experimental conditions.

Cell culture
Primary mouse renal tubular cells were isolated and cultured as previously described [37]. In brief, the kidneys were isolated from anesthetized mice and washed with PBS. After cutting into small pieces with scissors, the renal tissue was digested in 0.75 mg/mL type IV collagenase for 40 min at 37 °C. After filtration through a 100 μm strainer and collection by centrifugation at $1000 \times g$ at 4 °C for 5 min, the tubule fragments were washed three times with PBS, resuspended and plated in 60 mm dishes and cultured in 10% DMEM (Gibco, Grand Island, NY, USA) with 50 U/mL penicillin, 50 mg/mL streptomycin, and a hormone mix. Renal tubular cells were grown in dishes for 1 week. The first medium change was performed 3 days after cell plating, and was then changed every 2 days. Primary mouse renal tubular cells were transfected with Ad-KLF4 or Ad-shYAP (Hanbio Biotechnology, Shanghai, China). Whole-cell lysates were collected and subjected to Western blot and immunofluorescence analyses.

For the Transwell experiment, tubular cells were cultured in the upper compartment of a 0.4 μm Transwell plate. In addition, renal fibroblasts were cultured in the lower compartment. Ad-Ctrl, Ad-KLF4, and Ad-KLF4 + Ad-shYAP were transfected into tubular cells. The cell lysates of fibroblasts were collected and subjected to Western blot analysis.

Luciferase reporter assay
Primary tubular cells were transfected with Ad-Ctrl or Ad-KLF4. Twenty-four hours later, luciferase reporter plasmids containing the wild-type YAP promoter region (YAP WT) or a mutated YAP promoter region (YAP Mut), wild-type ITCH promoter region (ITCH WT) or a mutated ITCH promoter region (ITCH Mut) were transfected into tubular cells using Lipofectamine™ 2000 reagent(Invitrogen, Waltham, MA, USA). The cells were collected twenty-four hours after transfection. Then, the cells were analyzed by a dual luciferase reporter assay system (Promega, Madison, WI, USA). The luciferase activity of all groups was normalized to Renilla luciferase activity, and the differences between two groups were indicated as relative fold changes.

ChIP assay
Primary tubular cells were washed, cross-linked and sonicated. The cell lysates were subjected to immunoprecipitation with control IgG or antibodies. The immunoprecipitates were captured by protein A agarose/salmon sperm DNA. Phenol:chloroform extraction was used to isolate ChIP-enriched DNA. The target DNA was quantified by qPCR.

438

BrdU incorporation assay

Fibroblasts were cultured in DMEM containing 0.5% FBS (Gibco, Grand Island, NY, USA). The medium was replaced by BrdU test solution and incubated at 37 °C for 40 min. Then, the cells were washed three times with PBS and treated with methanol/acetic acid for 10 min followed by 0.3% H_2O_2–methanol for 30 min. After terminating the reaction with serum, DNA is denatured with formamide at 100 °C for 5 min, and the cells were washed with PBS for another three times and then incubated with anti-BrdU antibody (Abcam, Cambridge, MA, USA) for 1 h. Absorbance was measured on a TECAN Infinite M200 microplate reader (Salzburg Umgebung, Salzburg, Austria) at 370 nm.

Western blot analysis

The cells were washed with ice-cold PBS and lysed in cold RIPA buffer (Thermo Fisher Scientific, Waltham, MA, USA) with freshly added protease and phosphatase inhibitors using routine procedures. Total cell protein levels were determined by SDS-PAGE gels and blotted with the following antibodies: anti-KLF4 (ab106629, Abcam, Cambridge, MA, USA), anti-YAP (14074T, Cell Signaling Technology, Danvers, MA, USA), anti-P-YAP (13008S, Cell Signaling Technology, Danvers, MA, USA), anti-ITCH (ab108515, Abcam, Cambridge, MA, USA), anti-LATS1 (17049-1-AP, Proteintech, Chicago, IL, USA), anti-TGF-β (sc-130348, Santa Cruz Biotechnology, CA, USA), anti-CTGF (23936-1-AP, Proteintech, CHI, USA), anti-fibronectin (15613-1-AP, Proteintech, Chicago, IL, USA), anti-collagen I (14395-1-AP, Proteintech, Chicago, IL, USA), and anti-GAPDH (60004-1-lg, Proteintech, Chicago, IL, USA). Western blot results were quantified using ImageJ software. Statistical figures were drawn by GraphPad Prism 8.0 (San Diego, CA, USA).

Immunofluorescence

Primary mouse renal tubular cells were washed with PBS three times and fixed with stationary phase liquid for 15 min at room temperature. The cells were incubated overnight with primary antibodies at 4 °C, and then, the cells were incubated with secondary antibodies for 1 h at 37 °C, followed by incubation with DAPI (Sigma, St. Louis, MO, USA) for 10 min. The nuclei were stained with DAPI according to the manufacturer's instructions. Images were captured by confocal laser scanning biological microscopy (Leica, Wetzlar, Germany).

Quantitative RT-PCR

Total RNA was isolated using TRIzol reagent (Invitrogen, Waltham, MA, USA) according to the manufacturer's instructions in a routine procedure. Quantitative RT-PCR was performed with a Platinum SYBR Green qPCR Super Mix UDG kit (Invitrogen, Waltham, MA, USA). The sequences of the primers are listed in Table 1.

Statistical analyses

Statistical data were analyzed by using GraphPad Prism 8.0 (San Diego, CA, USA). Differences among groups and treatments for experiments were determined by one-way ANOVA. A P value < 0.05 was considered significant.

RESULTS

YAP is persistently increased and associated with renal deterioration after IR induction

Mice subjected to unilateral ischemia-reperfusion were used for the study of the AKI–CKD transition and related post-pathological alterations. As shown in Fig. 1a, the protein level of YAP increased by the 7th day after IR induction. On the 21st day after IR, the post-acute stage of AKI and YAP expression remained high (Fig. 1a). The real-time PCR results showed that the mRNA level of YAP was increased following the same pattern as the protein level (Fig. 1b).

To identify the effect of a continuous increase in YAP after IR, a recombinant adenovirus vector harboring the interference sequence targeting YAP (Ad-shYAP) was delivered to mice by intrarenal injection the 7th day after IR (Fig. 1c) [35]. The Western blot results showed that YAP expression was significantly suppressed by the 14th day after Ad-shYAP delivery. In addition, the increase in YAP expression after IR was significantly attenuated by Ad-shYAP (21st day after IR) (Fig. 1d). Immunohistochemistry data showed that knocking down YAP significantly attenuated the nuclear translocation of YAP after IR (Fig. 1e). Renal function was assessed by detecting the level of serum creatinine (Scr) and urinary ACR. Both serum Scr and urinary ACR were increased in the IR-treated mice. The IR-induced increase in Scr and urinary ACR was significantly attenuated by knocking down YAP (Fig. 1f, g). Renal morphological changes were detected by hematoxylin-eosin (H&E) staining. Ad-shYAP treatment significantly attenuated IR-induced renal morphological changes in the IR-treated mice (Fig. 1j), as characterized by reduced IR-induced renal tubule dilation, hyaline cast formation and epithelial cell atrophy, as well as interstitial inflammatory cell infiltration. The effect of YAP elevation on renal fibrosis after IR was also observed. The real-time PCR results showed that knocking down of YAP in the IR-treated mice reduced the upregulation of TGF-β and connective tissue growth factor (CTGF), which are regarded as the target molecules of the YAP signaling pathway and the pathogenic mediators in renal fibrosis (Fig. 1h, i). As shown in Fig. 1k, knocking down YAP reduced fibronectin and α-SMA expression after IR. These data suggest that a sustained increase in YAP level is related to renal dysfunction and the progression of fibrosis after IR.

The transcription factor KLF4 is persistently increased and associated with renal deterioration after IR induction

As shown in Fig. 2a, the KLF4 protein was increased on the 7th day after IR induction, and the increase was sustained to the 21st day, the progressive stage of fibrosis after AKI (Fig. 2a). The mRNA level of KLF4 was upregulated following the same pattern as the protein level (Fig. 2b). Immunohistochemistry data also showed that, compared with the sham group, the KLF4 levels were dramatically increased in the IR-treated mice, and KLF4 was mainly located in the nucleus of the renal tubular epithelial cells (Fig. 2c, d, red arrows).

To clarify the role of KLF4 after IR, a recombinant adenovirus vector harboring the interference sequence targeting KLF4 (Ad-shKLF4) or a control virus was delivered to mice by intrarenal injection. Ad-shKLF4 or Ad-Ctrl was administered on the 7th day

Table 1. Primer sequences for real-time PCR.

Gene	Sense	Antisense
KLF4	5′-CCAAGCCAAAGAGGGGAAGA-3′	5′-CGGTAGTGCCTGGTCAGTTCAT-3′
YAP	5′-CTGGGTGCCGTTTCTCCTG-3′	5′-CCATGTTGTTGTCTGATCGTTG-3′
TGF-β	5′-CCGCAACAACGCCATCTA-3′	5′-ACCAAGGTAACGCCAGGAAT-3′
CTGF	5′-TAGCCTCAAACTCCAAACACCA-3′	5′-GCTTTATCACCTGCACAGCATT-3′
GAPDH	5′-CAGGTTGTCTCCTGCGACTT-3′	5′-GGCCTCTCTTGCTCAGTGTC-3′

Sustained activation of KLF4-YAP promotes renal fibrosis
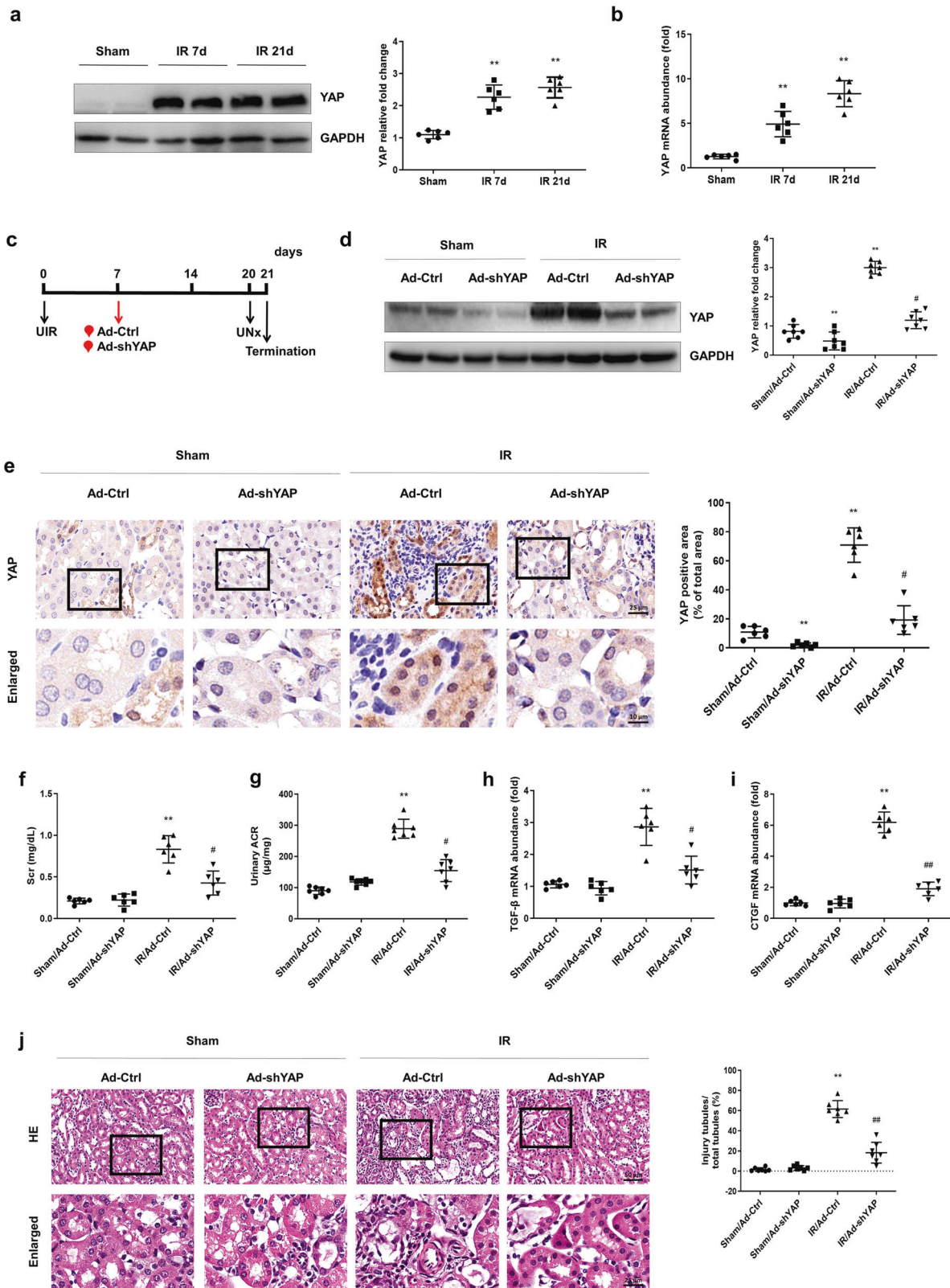D Xu et al.

439

Fig. 1 (continued)

after IR surgery (Fig. 2e). The Western blot and PCR analyses revealed that KLF4 was almost abolished by the 14th day after Ad-shKLF4 delivery. Ad-shKLF4 treatment alleviated the IR-induced increase in KLF4 (on the 21st day after IR) (Fig. 2f, g). The increase

in Scr and urinary ACR levels in the IR-treated mice was significantly blunted by knocking down KLF4 (Fig. 2h, i). The H&E staining results also showed that knocking down KLF4 significantly attenuated tubule dilation, hyaline cast
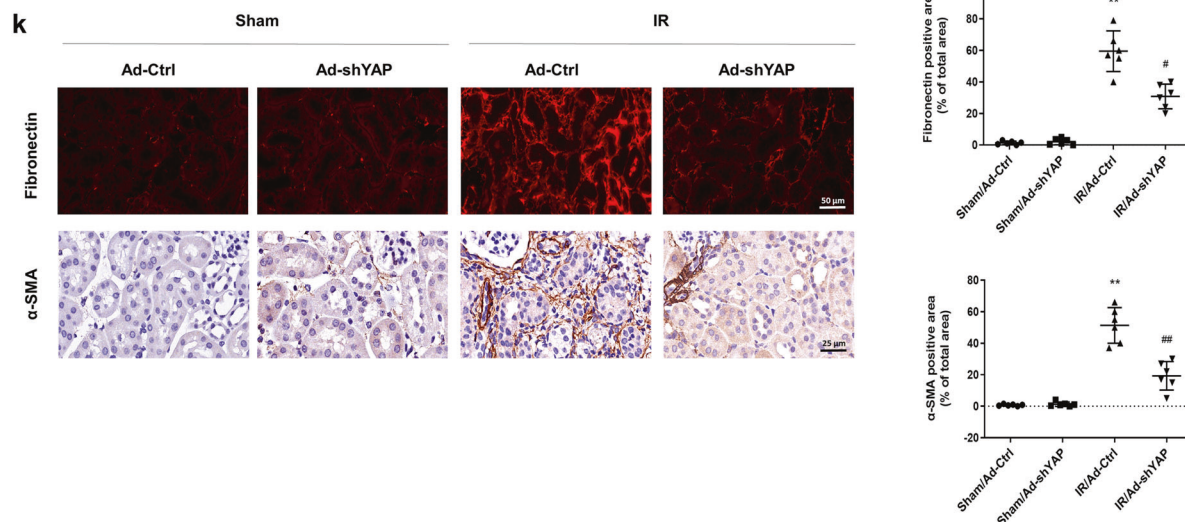
Sustained activation of KLF4-YAP promotes renal fibrosis
D Xu et al.

440

Fig. 1 **A sustained increase in YAP is associated with renal deterioration after IR induction. a** Western blotting was conducted to detect the protein level of YAP on the 7th and 21st days after IR induction. **b** Real-time PCR was conducted to determine the mRNA level of KLF4 on the 7th and 21st days after IR. $n = 6$ mice in each group. Data are presented as the means $\pm$ SEM. $**P < 0.01$ versus the sham group. **c** Experimental scheme. The red arrow indicates the injection of the Ad-Ctrl or Ad-shYAP adenovirus. Black arrows indicate the timing of the renal IR surgery. **d** Western blotting was conducted to determine the protein level of YAP in the four groups as indicated. **e** IHC was performed to visualize the distribution of YAP in different groups of mice as indicated. Boxed areas are enlarged and presented in the figures below. Quantitative analyses of the YAP-positive area for the four groups as indicated. At least ten randomly selected fields were evaluated for each kidney. **f** The level of serum creatinine (Scr) was determined for the four groups as indicated. **g** Urinary ACR values were calculated. The mRNA levels of TGF-β (**h**) and CTGF (**i**) were determined for the four groups as indicated. **j** Kidney sections were subjected to H&E staining. Boxed areas are enlarged and presented in the figures below. Quantitative analyses of injured tubules in the four groups as indicated. **k** Representative images of immunostained samples show fibronectin and α-SMA expression for the four groups. $n = 6$ mice in each group. Data are presented as the means $\pm$ SEM. $**P < 0.01$ versus the sham/Ad-Ctrl group. $^{#}P < 0.05$, $^{##}P < 0.01$ versus the IR/Ad-Ctrl group. IR ischemia-reperfusion, UNx unilateral nephrectomy, ACR albmine to creatinine ratio, IHC immunohistochemistry.

formation, epithelial cell atrophy and interstitial inflammatory cell infiltration after IR (Fig. 2j). These data indicate that the sustained increase in the transcription factor KLF4 is also associated with renal pathological changes and functional decline after IR.

KLF4 promotes renal fibrosis after IR induction by upregulating YAP expression
The relationship between KLF4 and increased YAP in IR-induced chronic renal dysfunction was further investigated. As shown in Fig. 3a, the Western blot results showed that knocking down KLF4 reversed the upregulation of YAP expression on the 21st day after IR induction. As shown in Fig. 3b, c, the PCR results showed that treatment with Ad-shKLF4 after IR attenuated the upregulation of TGF-β and CTGF. As shown in Fig. 3d, knocking down KLF4 inhibited the IR-induced expression of TGF-β and CTGF. The immunohistochemistry results showed that knocking down KLF4 reduced the nuclear translocation of YAP in the IR-treated mice (Fig. 3e). Masson's staining showed that knocking down KLF4 attenuated renal fibrotic lesions on the 21st day after IR (Fig. 3f). Similar results were observed when kidney sections were stained with antibodies against fibronectin and α-SMA (Fig. 3g). As shown in Supplementary Fig. S2, the overexpression of KLF4 induced renal fibrosis 2 weeks after Ad-KLF4 transfection. These data suggested that the increase in KLF4 was related to the increase in YAP expression, nuclear translocation and progression of fibrosis after IR.

Overexpression of KLF4 aggravates YAP elevation and renal injury in the IR-treated mice
To further identify the causative link between KLF4 and YAP in IR-induced renal fibrosis, Ad-KLF4 or Ad-KLF4 + Ad-shYAP was administered to the mice on the 7th day after IR induction

(Fig. 4a). As shown in Fig. 4b, the Western blot results showed that the overexpression of KLF4 aggravated the increase in YAP expression in the IR-treated mice, and this was suppressed by YAP knockdown. The renal function deterioration indicators Scr and urinary ACR were further increased in the IR-treated mice after KLF4 was overexpressed. Knocking down YAP inhibited the Ad-KLF4-induced increases in Scr and urinary ACR (Fig. 4c, d). The PCR results also showed that the mRNA levels of CTGF and TGF-β were further upregulated in Ad-KLF4-treated mice compared with those of the IR-treated mice but were inhibited upon administration of Ad-shYAP (Fig. 4e, f). The Western blot results also showed that the YAP knockdown attenuated the KLF4-overexpression-induced upregulation of CTGF and TGF-β protein levels (Fig. 4g). As shown in Fig. 4h, the overexpression of KLF4 exacerbated interstitial collagen and fibronectin deposition and intensified the α-SMA positive staining in the IR-treated mice, which the effects were attenuated by YAP knockdown. These data also implicated the upregulation of KLF4 in the development of renal fibrosis after IR surgery by upregulating YAP expression.

KLF4 transcriptionally regulates the expression of YAP in primary cultured tubular cells
In primary cultured renal tubular cells, the overexpression of KLF4 upregulated the protein level of YAP (Fig. 5a). Consistently, real-time PCR results indicated that the transfection of Ad-KLF4 significantly induced an increase in YAP mRNA levels (Fig. 5b). Using the JASPAR database (http://jaspar.genereg.net/), a bioinformatics analysis was conducted, and the results revealed a computationally KLF4-binding site in the YAP promoter region (Fig. 5c). To identify the link between KLF4 and YAP, a reconstructed luciferase vector harboring wild-type (WT) *YAP* or *YAP* with a mutated promoter region was cotransferred into

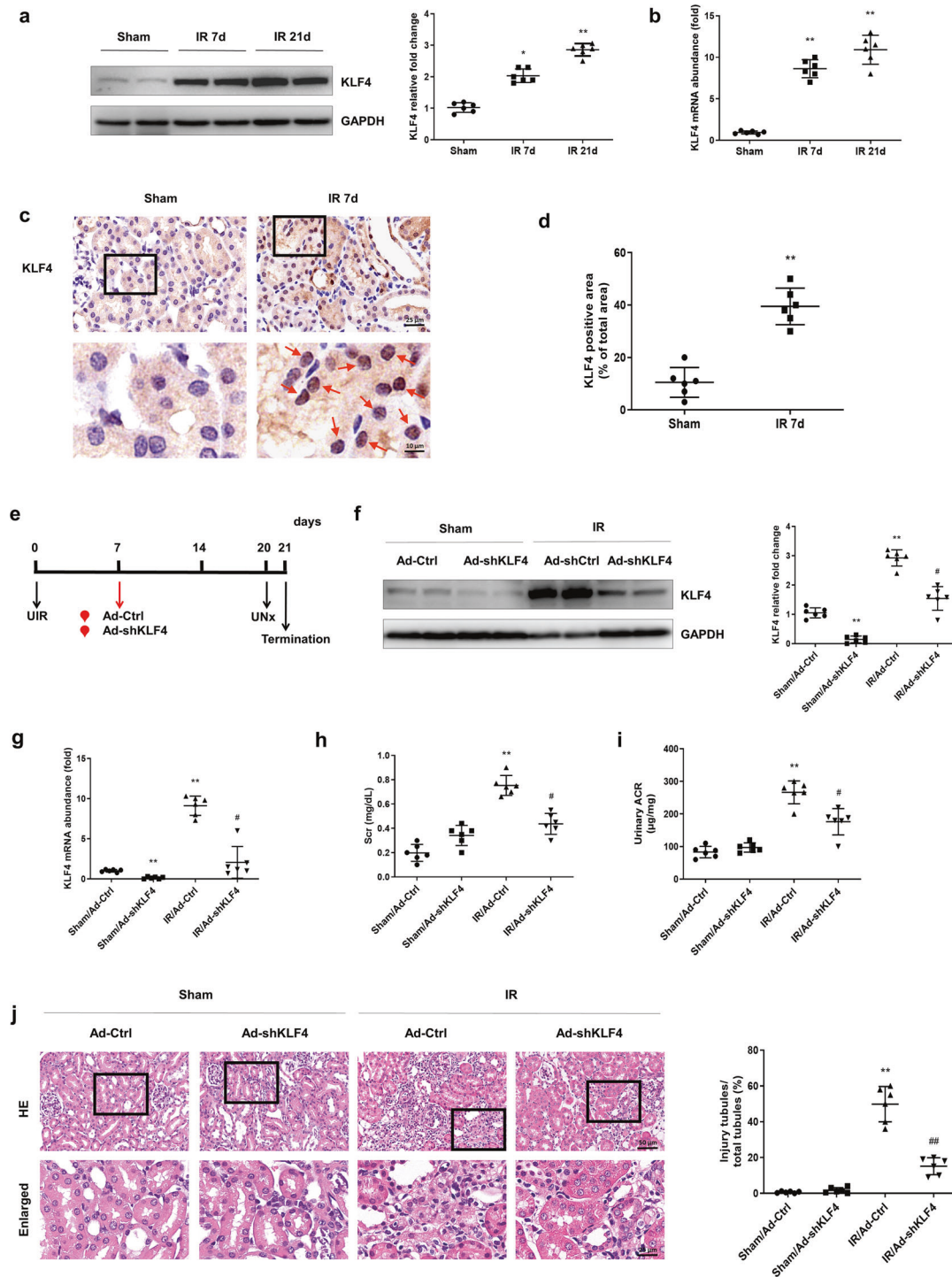Sustained activation of KLF4-YAP promotes renal fibrosis
D Xu et al.

441

Fig. 2   The transcription factor KLF4 is persistently increased after IR induction. a Western blotting was conducted to detect the protein level of KLF4 on the 7th and 21st days after IR induction. **b** Real-time PCR was conducted to determine the mRNA level of KLF4 on the 7th and 21st days after IR. **c** IHC was performed to visualize the distribution of KLF4 in the two groups of mice. Red arrows indicate KLF4-positive tubules. **d** Quantitative analyses of the KLF4-positive area for the two groups as indicated. At least ten randomly selected fields were evaluated for each kidney. $n = 6$ mice in each group. Data are presented as the means ± SEM. *$P < 0.05$, **$P < 0.01$ versus the sham group. **e** Experimental scheme. The red arrow indicates the injection of the Ad-Ctrl or Ad-shKLF4 adenovirus. Black arrows indicate the timing of the renal IR surgery. **f** Western blotting was conducted to determine the level of KLF4 protein in the four groups. **g** The mRNA level of KLF4 was determined for the four groups. **h** The level of Scr was determined for the four groups. **i** Urinary ACR values were calculated for the four groups. **j** Kidney sections were subjected to H&E staining. Boxed areas are enlarged and presented in the figures below. Quantitative analyses of the injured tubules in the four groups. $n = 6$ mice in each group. Data are presented as the means ± SEM. **$P < 0.01$ versus the sham/Ad-Ctrl group. #$P < 0.05$, ##$P <$ 0.01 versus the IR/Ad-Ctrl group. IR ischemia-reperfusion, UNx unilateral nephrectomy, ACR albumine to creatinine ratio, IHC immunohistochemistry.
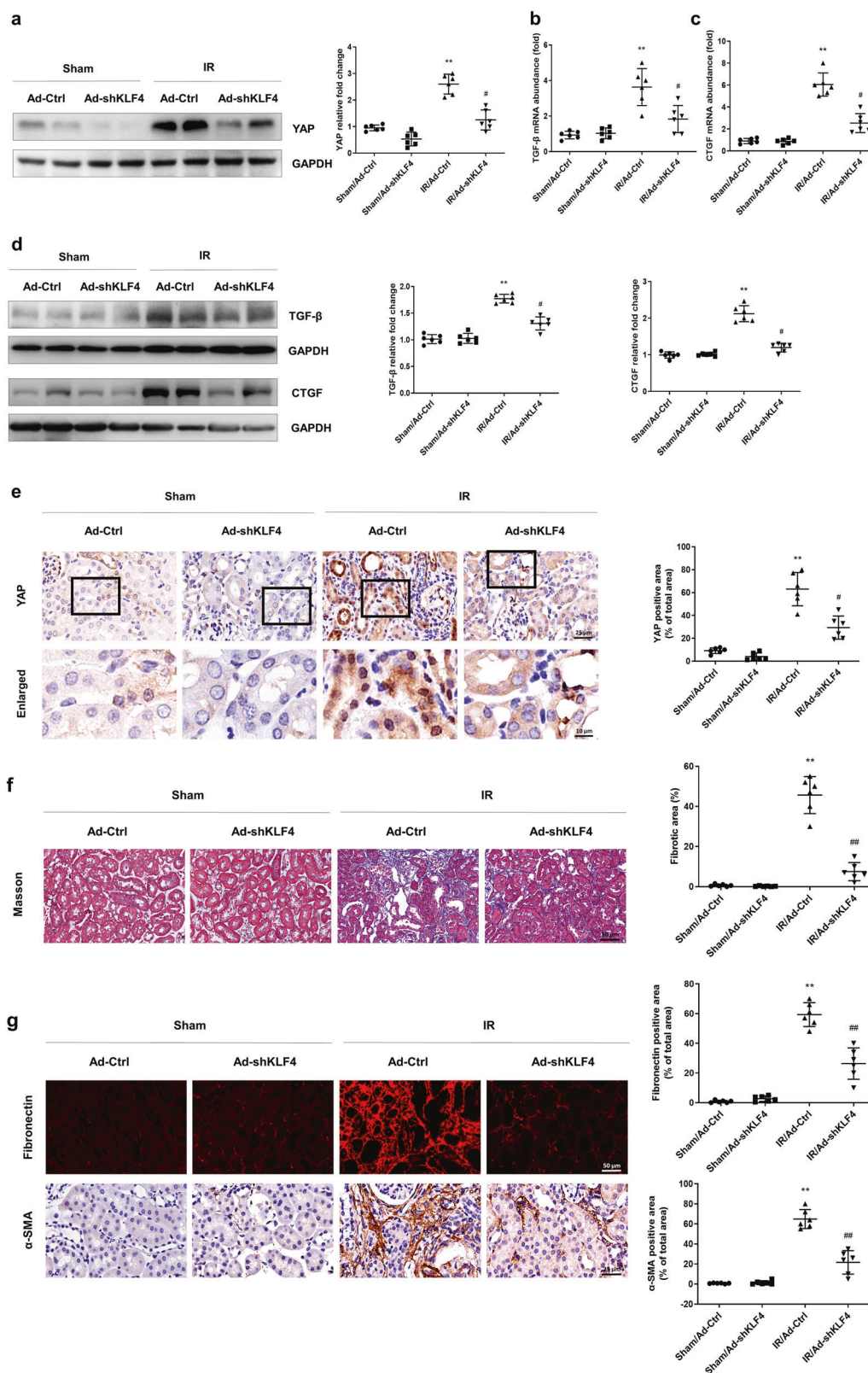
Sustained activation of KLF4-YAP promotes renal fibrosis
D Xu et al.

442

Fig. 3 **KLF4 promotes progressive renal fibrosis after IR induction by upregulating YAP expression. a** Western blotting was conducted to detect the protein level of YAP in the four groups as indicated. The mRNA levels of TGF-β (**b**) and CTGF (**c**) were determined for the four groups as indicated. **d** Western blotting was conducted to determine the protein levels of TGF-β and CTGF in the four groups as indicated. **e** IHC was performed to visualize the distribution of YAP. Boxed areas are enlarged and presented in the figures below. Quantitative analyses of the YAP-positive area for the four groups as indicated. **f** Masson's trichrome staining was used to detect collagen deposition in the four groups. Quantitative analyses of the extent of fibrosis. **g** Representative immunostaining images show fibronectin and α-SMA expression in the four groups. $n = 6$ mice in each group. Data are presented as the means ± SEM. **$P < 0.01$ versus the sham/Ad-Ctrl group. #$P < 0.05$, ##$P < 0.01$ versus the IR/Ad-Ctrl group, IR ischemia-reperfusion, IHC immunohistochemistry.

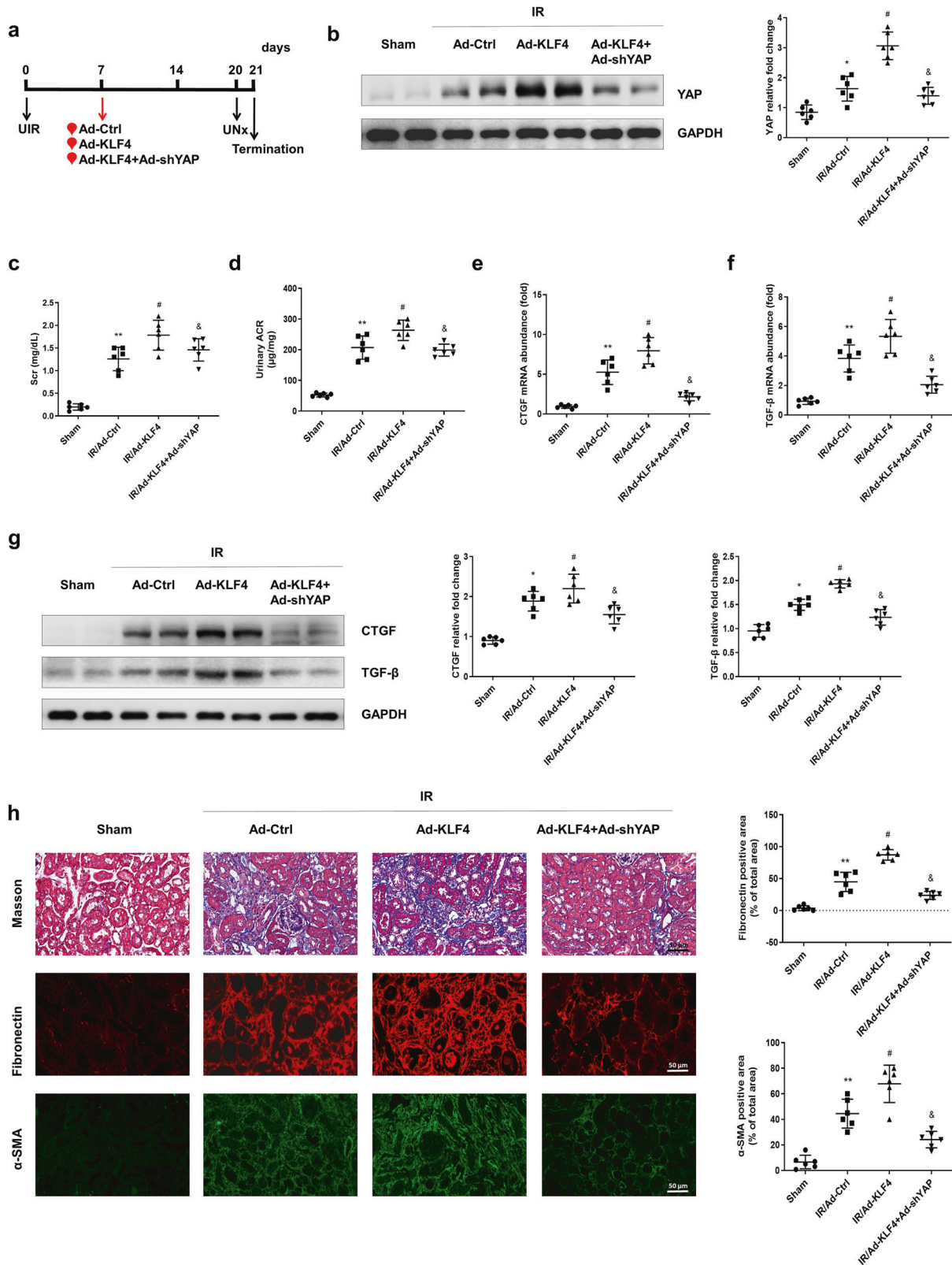Sustained activation of KLF4-YAP promotes renal fibrosis
D Xu et al.

443

Fig. 4 Overexpression of KLF4 aggravates YAP-mediated renal injury after IR induction. a Experimental scheme. The red arrow indicates the injection of the Ad-Ctrl, Ad-KLF4 or Ad-KLF4 + Ad-shYAP adenovirus. Black arrows indicate the timing of the renal IR surgery. **b** Western blotting was conducted to determine the protein level of YAP in the four groups as indicated. **c** The level of serum creatinine (Scr) was determined for the four groups. **d** Urinary ACR values were calculated. The mRNA levels of CTGF (**e**) and TGF-β (**f**) were determined for the four groups. **g** Western blotting was conducted to determine the protein levels of CTGF and TGF-β in the four groups, as indicated. **h** Kidney sections were subjected to Masson's staining. Representative images of immunostained samples showing fibronectin and α-SMA expression in the three groups. $n = 6$ mice in each group. Data are presented as the means ± SEM. *$P < 0.05$, **$P < 0.01$ versus the sham group. #$P < 0.05$ versus the IR/Ad-Ctrl group. &$P < 0.05$ versus the IR/Ad-KLF4 group. IR ischemia-reperfusion, UNx unilateral nephrectomy, ACR albumine to creatinine ratio.

Sustained activation of KLF4-YAP promotes renal fibrosis
D Xu et al.

444

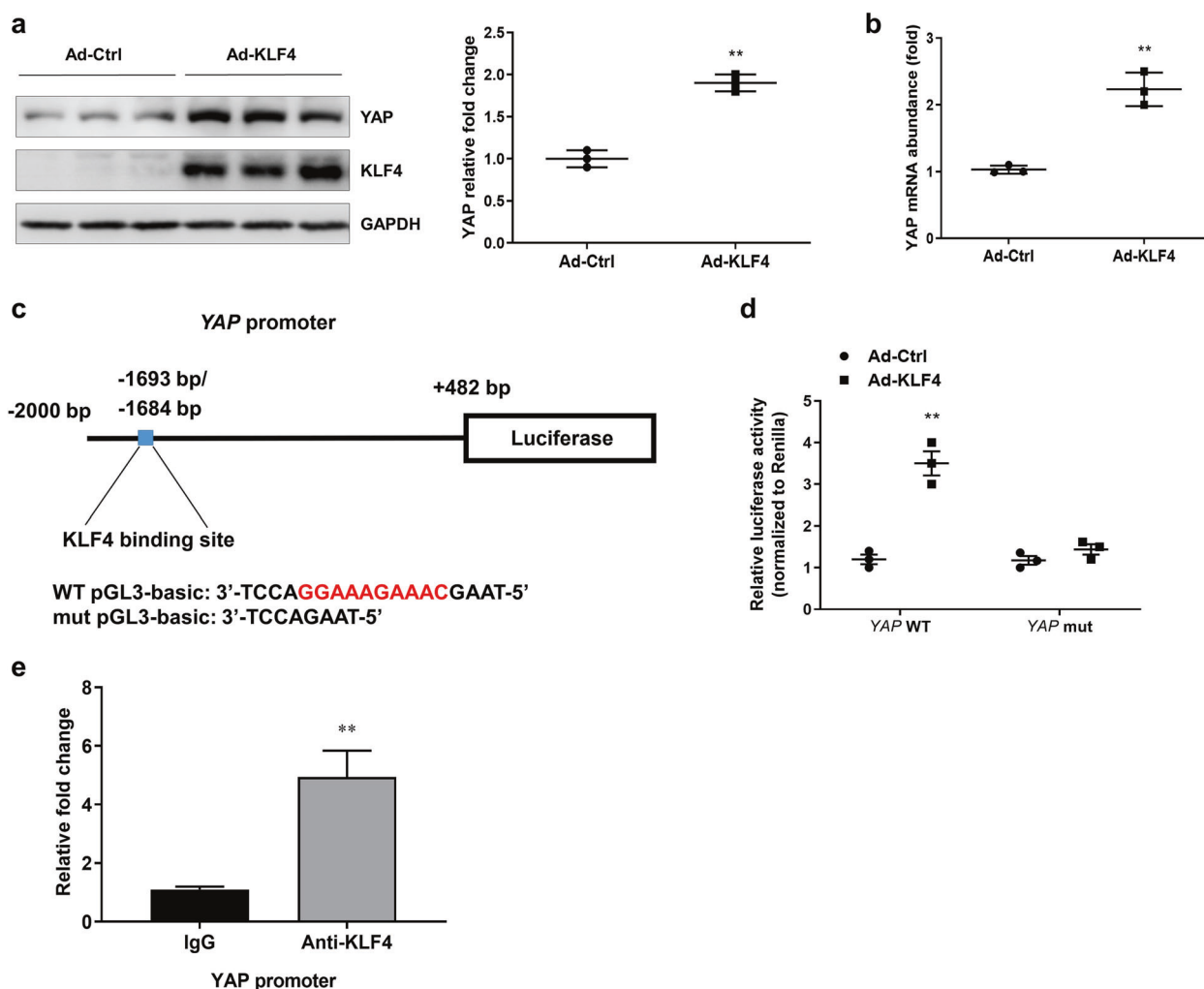**Fig. 5 KLF4 transcriptionally regulates the expression of YAP in primary cultured tubular cells. a** Expression of KLF4 and YAP in primary tubular cells transfected with Ad-Ctrl and Ad-KLF4 for 24 h was assessed by Western blotting. **b** The mRNA level of YAP was determined by real-time PCR. **c** Experimental scheme showing luciferase expression construct with the YAP promoter region. Base pair (bp) numbers indicate positions relative to the YAP transcription start site. The blue box indicates the KLF4-binding motif; the genomic sequence of WT pGL3-basic vector is shown below. Mutant YAP promoter construct with a 10-bp deletion (red region) at the pGL3-basic site (mut pGL3-basic). **d** Luciferase expression analysis based on wild-type and mutant YAP promoter regions in primary tubular cells 1 day after transfection with Ad-Ctrl or Ad-KLF4. Data are presented as the means ± SEM. **$P < 0.01$ versus the Ad-Ctrl group. **e** KLF4 binding to the promoter of YAP as determined by chromatin immunoprecipitation assay. The regions with the KLF4-binding sites were quantified and normalized to the levels of the IgG pull-down assay. Data are presented as the means ± SEM. **$P < 0.01$ compared with IgG control. $n = 3$ experimental replicates.

primary cultured tubular cells with Ad-Ctrl or Ad-KLF4, 24 h after cotransfecttion, a luciferase assay was used to examine the link between KLF4 and YAP. The transfection of Ad-KLF4 significantly increased luciferase activity. The mutation in the YAP promoter region by deleting KLF4 binding site (YAP mut) abolished the effect of the Ad-KLF4 transfection (Fig. 5d). A chromatin immunoprecipitation assay was performed to determine whether KLF4 was bound directly to the promoter region of YAP. As shown in Fig. 5e, significant enrichment of the chromatin region was detected in the anti-KLF4 group compared with that of the IgG control group. These data indicate that KLF4 was able to bind to the promoter region of YAP and positively regulate YAP expression.

KLF4 promotes the nuclear translocation of YAP by transcriptionally enhancing ITCH expression
P-YAP remains in the cytoplasm and is activated by dephosphorylation. LATS1, a serine/threonine kinase, plays a key role in phosphorylating YAP, while ITCH negatively regulates YAP phosphorylation by enhancing the degradation of LATS1. Using the JASPAR database (http://jaspar.genereg.net/), a bioinformatics analysis was conducted, and the results revealed a computationally KLF4-binding site in the ITCH promoter region (Fig. 6c). To investigate the underlying mechanism of YAP nuclear translocation, KLF4 was overexpressed in primary cultured renal tubular cells upon transfection with Ad-KLF4. The Western blot results indicated that the overexpression of KLF4 significantly increased the expression of ITCH and reduced the levels of LATS1 and P-YAP (Fig. 6a). These results were confirmed by immunofluorescence assay. As shown in Fig. 6b, the transfection of Ad-KLF4 increased the expression of ITCH, which was mainly located in the cytoplasm. To identify the link between KLF4 and ITCH, a reconstructed luciferase vector harboring wild-type (WT) ITCH or ITCH with a mutated promoter region was cotransferred into primary cultured tubular cells with Ad-Ctrl or Ad-KLF4. Twenty-four hours after the cotransfection, a luciferase assay was used to examine the link between KLF4 and ITCH. As shown in Fig. 6d, cotransfection of the ITCH WT luciferase vector with Ad-KLF4

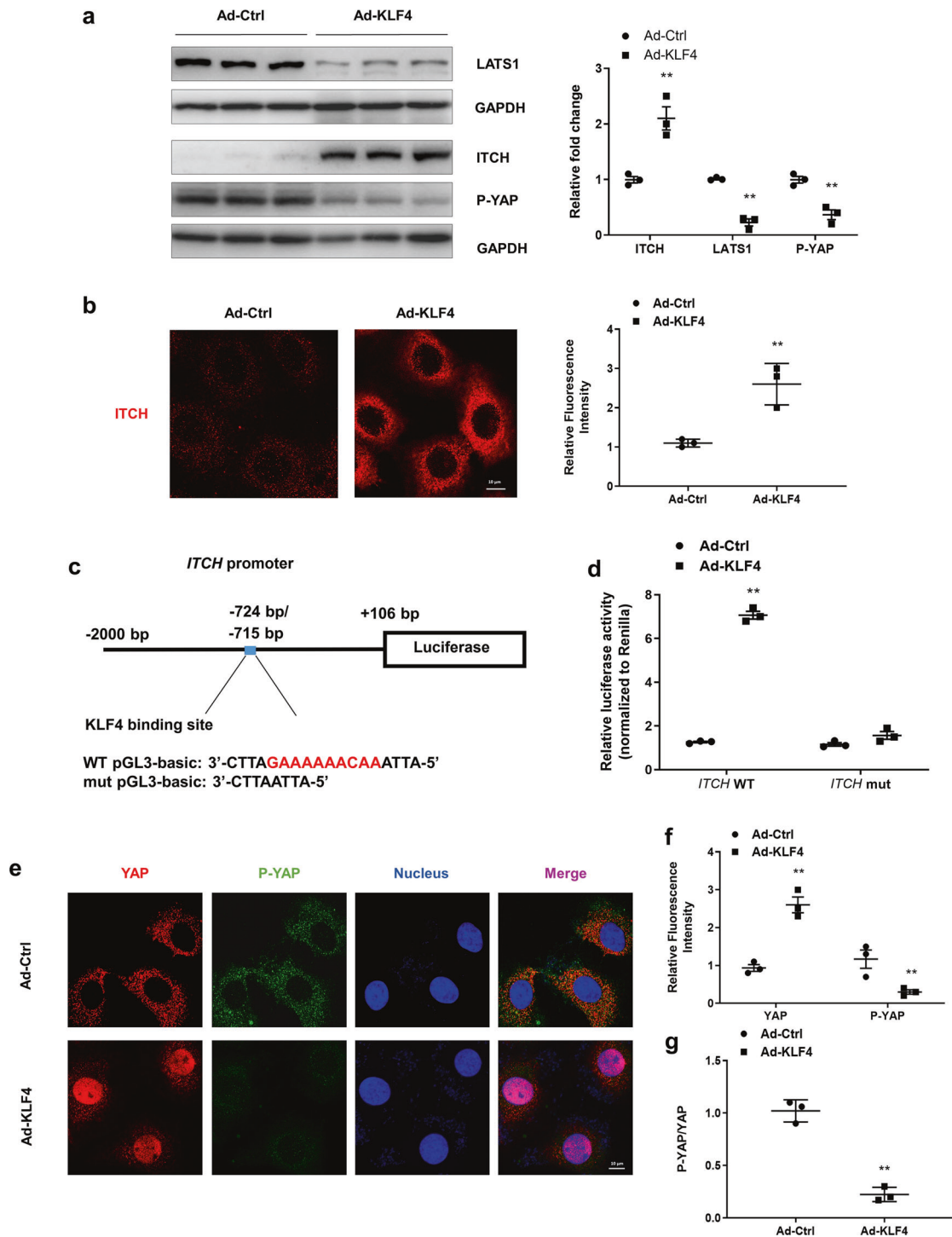Sustained activation of KLF4-YAP promotes renal fibrosis
D Xu et al.

445

Fig. 6 KLF4 promotes YAP nuclear translocation by transcriptional regulation of ITCH expression. a The expression of ITCH, LATS1 and P-YAP in primary tubular cells transfected with Ad-Ctrl and Ad-KLF4 for 24 h was assessed by Western blotting. **b** Representative images of the primary tubular cells after transfection with Ad-Ctrl and Ad-KLF4 immunostained for ITCH (red). **c** Experimental scheme showing luciferase expression construct with the ITCH promoter region. Base pair (bp) numbers indicate positions relative to the ITCH transcription start site. The blue box indicates the KLF4-binding motif; the genomic sequence of WT pGL3-basic vector is shown below. Mutant ITCH promoter construct with a 10-bp deletion (red region) in the pGL3-basci site (mut pGL3-basci). **d** Luciferase expression analysis based on the wild-type and mutant ITCH promoter regions in the tubular cells 24 h after transfection with Ad-Ctrl or Ad-KLF4. **e** Representative images of the primary tubular cells immunostained for YAP (red), P-YAP (green), and nucleus (blue) after transfection with Ad-Ctrl or Ad-KLF4. **f** Quantitative analyses of the positive fluorescence staining of YAP and P-YAP in the two groups. **g** The ratio of P-YAP and YAP was calculated. $n = 3$ experimental replicates. Data are presented as the means ± SEM. **$P < 0.01$ versus the Ad-Ctrl group.

increased the luciferase activity. The mutation of the *ITCH* promoter region in which KLF4-binding site was deleted (*ITCH* mut) abrogated the effect of Ad-KLF4 cotransfection. Moreover, the immunofluorescence results showed that overexpression of KLF4 induced a significant increase in the nuclear translocation of YAP and a decrease in P-YAP (Fig. 6e, f). The ratio of P-YAP to YAP was significantly decreased after Ad-KLF4 transfection, indicating the activation of YAP (Fig. 6g). In addition, knocking down ITCH reversed the Ad-KLF4-induced decrease in P-YAP/YAP in the renal tubular cells (Supplementary Fig. S3). These data suggested that KLF4 facilitated YAP nuclear translocation by positively regulating ITCH expression and then enhancing LATS1 degradation.

KLF4-induced YAP activation is implicated in the communication between tubular cells and interstitial fibroblasts
The activation of renal interstitial fibroblasts plays an essential role in renal interstitial fibrosis. Fibrogenic factors originally secreted by tubular epithelial cells, such as TGF-β and CTGF, are important in triggering interstitial fibroblast activation. In the Transwell coculture system (Fig. 7a), the effect of KLF4-initiated YAP elevation in the tubular epithelial cells promoting fibroblast activation was evaluated. As shown in Fig. 7b, c, in the primary cultured renal tubular epithelial cells, transfection of Ad-KLF4 significantly increased YAP expression. Cotransfection of Ad-shYAP effectively suppressed the Ad-KLF4-induced increase in YAP. Overexpression of KLF4 increased the production of TGF-β and CTGF. Cotransfection of Ad-shYAP with Ad-KLF4 significantly inhibited the expression of TGF-β and CTGF (Fig. 7d–f). For the cell lysate of the fibroblasts, the Western blot results indicated that the overexpression of KLF4 in tubular cells enhanced the expression of fibronectin and collagen I in the fibroblasts (Fig. 7g–i). Moreover, cotransfection of Ad-KLF4 with Ad-shYAP into the tubular cells significantly attenuated the increases in fibronectin and collagen I in the fibroblasts. Bromodeoxyuridine (BrdU) incorporation assays were used to determine fibroblast proliferation. The overexpression of KLF4 in the tubular cells induced an increase in fibroblast proliferation, which was suppressed by YAP knockdown (Fig. 7j). These findings suggest that KLF4 was critical for the interaction between tubular cells and fibroblasts. Elevated KLF4-induced YAP activation promoted renal interstitial fibroblast activation.

Elevated KLF4 is critical for the YAP activation in AKI-CKD mice
The Western blot results showed that the expression of ITCH was increased on the 7th day after IR induction and were maintained at a high level to the 21st day after IR. In contrast, LATS1 exhibited a sustained decrease (Fig. 8a). To investigate the role of KLF4 in YAP dephosphorylation and nuclear translocation, Ad-shKLF4 or Ad-Ctrl was administered to the mice by intrarenal injection on the 7th day after IR. Knocking down KLF4 reversed the IR-induced upregulation of ITCH and downregulation of LATS1 on the 21st day after IR (Fig. 8b). The immunohistochemistry results showed that LATS1 was mainly located in the renal tubules. Knocking down KLF4 restored the IR-induced decrease in LATS1 (Fig. 8c). To determine the activation of YAP, the ratio of P-YAP/YAP was determined. The Western blot results showed that KLF4 knockdown reversed the IR-induced decrease in P-YAP/YAP (Fig. 8d). These data suggested that KLF4 was involved in YAP activation.

YAP increases during clinical nephropathy development and is associated with renal fibrosis
To test the clinical relevance of YAP in the pathogenesis of CKD, immunohistochemistry staining was carried out in kidney biopsy specimens obtained from patients. YAP was negligibly detected in the normal human kidney samples, while the signal for YAP was dramatically increased in all the biopsy specimens from the patients with CKD (Fig. 9a) and was predominantly localized in the nucleus of renal tubular epithelial cells (Fig. 9a, red arrows). In addition, YAP expression was related to renal fibrosis (Fig. 9b).

DISCUSSION
AKI has been recognized as an important issue in inducing CKD and renal fibrosis, while the incidence of IR-induced AKI continues to increase in the clinic [7, 38, 39]. On the IR-induced AKI to CKD animal model, our results demonstrated that sustained activation of YAP in the post-acute phase of AKI was involved in renal function decline and interstitial fibrosis.

A previous study reported that YAP promoted UUO-induced renal fibrosis by mechanoregulating the TGF-β-smad signaling pathway, which led to fibroblast transformation and ECM production [40]. In this manuscript, we characterized that YAP activation in renal tubular epithelial cells after IR induction. YAP activation was previously shown to play a protective role in mediating epithelial cell regeneration during kidney recovery from AKI. For the related experiment, our results showed that expression of YAP, the central effector in the Hippo signaling pathway, was sustainably increased during the acute phase until 3 weeks after IR induction in the mice. Knocking down YAP after the acute phase of AKI attenuated renal function decline and interstitial fibrosis, which suggests that the sustained activation of YAP in the post-acute phase of AKI is involved in chronic renal deterioration after AKI.

The relationship between tubular epithelial cells and interstitial fibrosis plays an important role in promoting fibrosis [41, 42]. Cytokines released by injured tubular epithelial cells initiate the activation of interstitial fibroblasts and tissue repair [41, 43–46]. As a conserved pathway in regulating cell differentiation and proliferation, the Hippo pathway targets the profibrotic factors TGF-β and CTGF. For the related experiment, our results showed that combined with the increase in YAP expression, both TGF-β and CTGF expression was increased significantly in the tubular epithelial cells. Knocking down YAP suppressed the increase in TGF-β and CTGF, which suggests that the elevation of YAP is related to the increase in the profibrotic response.

The activation of interstitial fibroblasts plays a central role in renal fibrosis. Renal tubular epithelial cells are major sources of TGF-β and CTGF under pathological conditions. For the related experiment with the Transwell system, the results demonstrated that TGF-β and CTGF originating from tubular epithelial cells were able to trigger the activation of fibroblasts. Thus, increasing the expression and secretion of TGF-β and CTGF from renal tubular epithelial cells might be the mechanism for sustaining the activation of YAP that triggers the activation of interstitial fibroblasts and promotes renal fibrosis.

In another experiment, we also observed that the reprogramming factor KLF4 was aligned upstream of YAP and was critical for the upregulation and activation of YAP after IR induction. The reprogramming factor involved in the pathogenesis of the kidney is not a trivial concern [5, 47]. In our previous study, we observed that the reprogramming factor c-Myc was implicated in renal fibrosis because it facilitates TGF-β activation [48]. For the in vivo and in vitro experiments, our results suggest that both YAP and ITCH are downstream target genes of KLF4. Therefore, KLF4 upregulated the expression of YAP and increased the activation of YAP by upregulating the expression of ITCH.

ITCH does not activate YAP directly. Phosphorylated YAP is the inactive form and remains in the cytoplasm. The phosphorylation of YAP depends on LATS1, a serine/threonine kinase in the Hippo signaling pathway [49]. As an E3 ubiquitin protein ligase, ITCH facilitates the degradation of LATS1 via polyubiquitination. In the experiment, our results showed that the expression of ITCH followed a similar pattern to that of KLF4, while the expression of LATS1 showed the opposite pattern. ITCH was persistently increased after IR, and LATS1 was continuously decreased. Knockdown of KLF4 attenuated the increase in ITCH and decrease in LATS1. At the same time, the nuclear translocation of YAP was inhibited by KLF4 knockdown and aggravated by KLF4 overexpression. This is consistent with results from other groups, suggesting that the
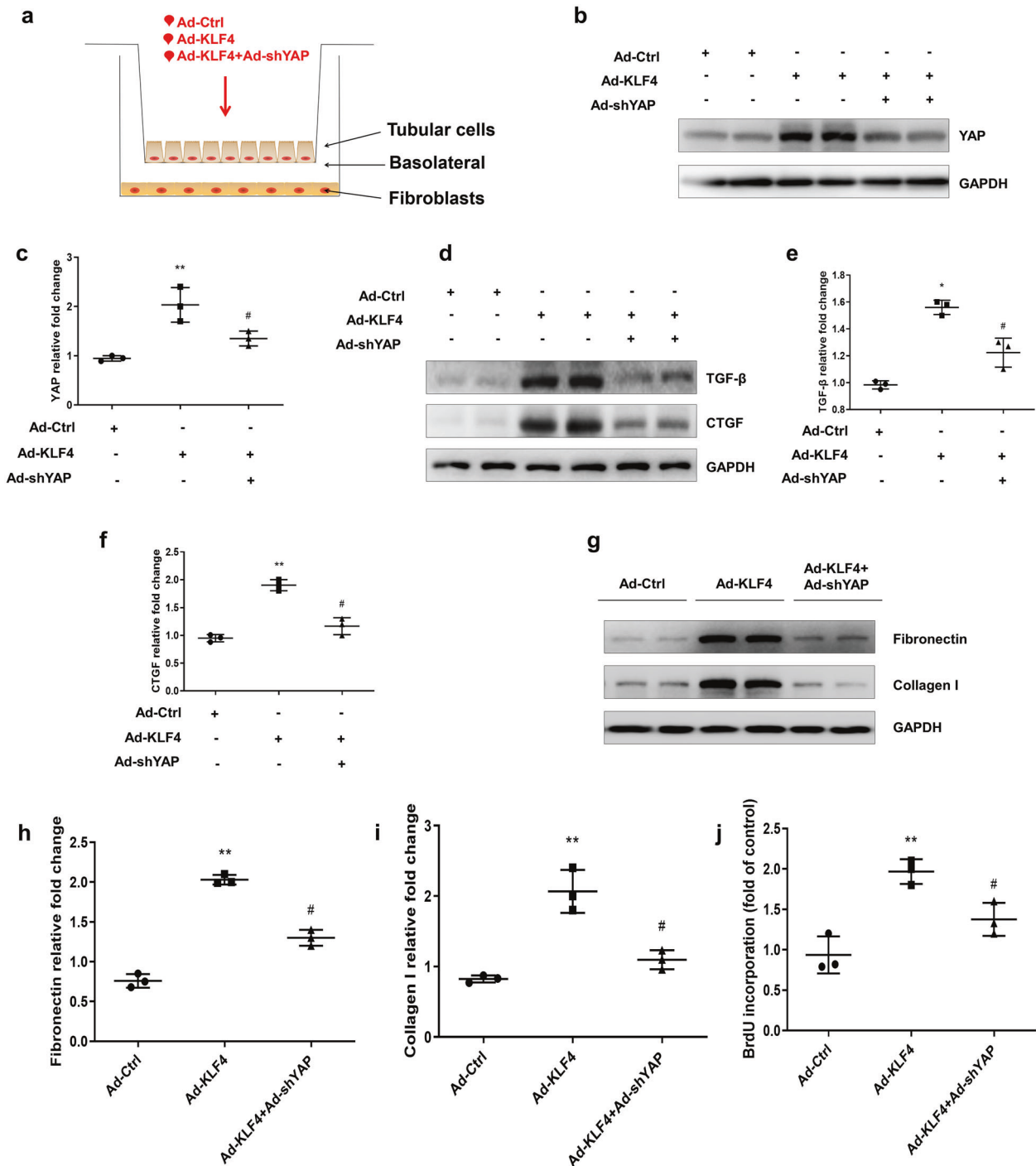
Sustained activation of KLF4-YAP promotes renal fibrosis
D Xu et al.

447

Fig. 7 KLF4-induced YAP activation is associated with communication between tubular cells and interstitial fibroblasts. a Scheme showing the Transwell experiment results with primary tubular cells and fibroblasts. Primary tubular cells were transfected with three groups of adenovirus vectors (Ad-Ctrl, Ad-KLF4, or Ad-KLF4 + Ad-shYAP) as indicated. **b** Representative Western blots show the protein level of YAP in the cell lysate of tubular cells. **c** Quantitative analyses of YAP in the three groups. **d** Representative Western blots show that Ad-shYAP inhibits KLF4-induced TGF-β and CTGF expression. Quantitative analyses of TGF-β (**e**) and CTGF (**f**) in the three groups. **g** For the cell lysate of fibroblasts, representative Western blots show fibronectin and collagen I expression. Quantitative analyses of fibronectin (**h**) and collagen I (**i**) in the three groups. **j** Fibroblast proliferation was measured by BrdU incorporation assay. $n = 3$ experimental replicates. Data are presented as the means ± SEM. *$P < 0.05$, **$P < 0.01$ versus the Ad-Ctrl group. #$P < 0.05$ versus the Ad-KLF4 group.

change in ITCH abundance alone is sufficient for altering LATS1-YAP-mediated downstream signaling and the regulation of tumor cell proliferation. All these results suggested that the nuclear translocation of YAP was regulated by KLF4 via the expression of ITCH.

Taken together, the results demonstrated that the sustained activation of YAP, a beneficial factor in facilitating renal repair in AKI, displays a negative effect in the post-acute phase after IR injury. Sustained activation of YAP increases the expression
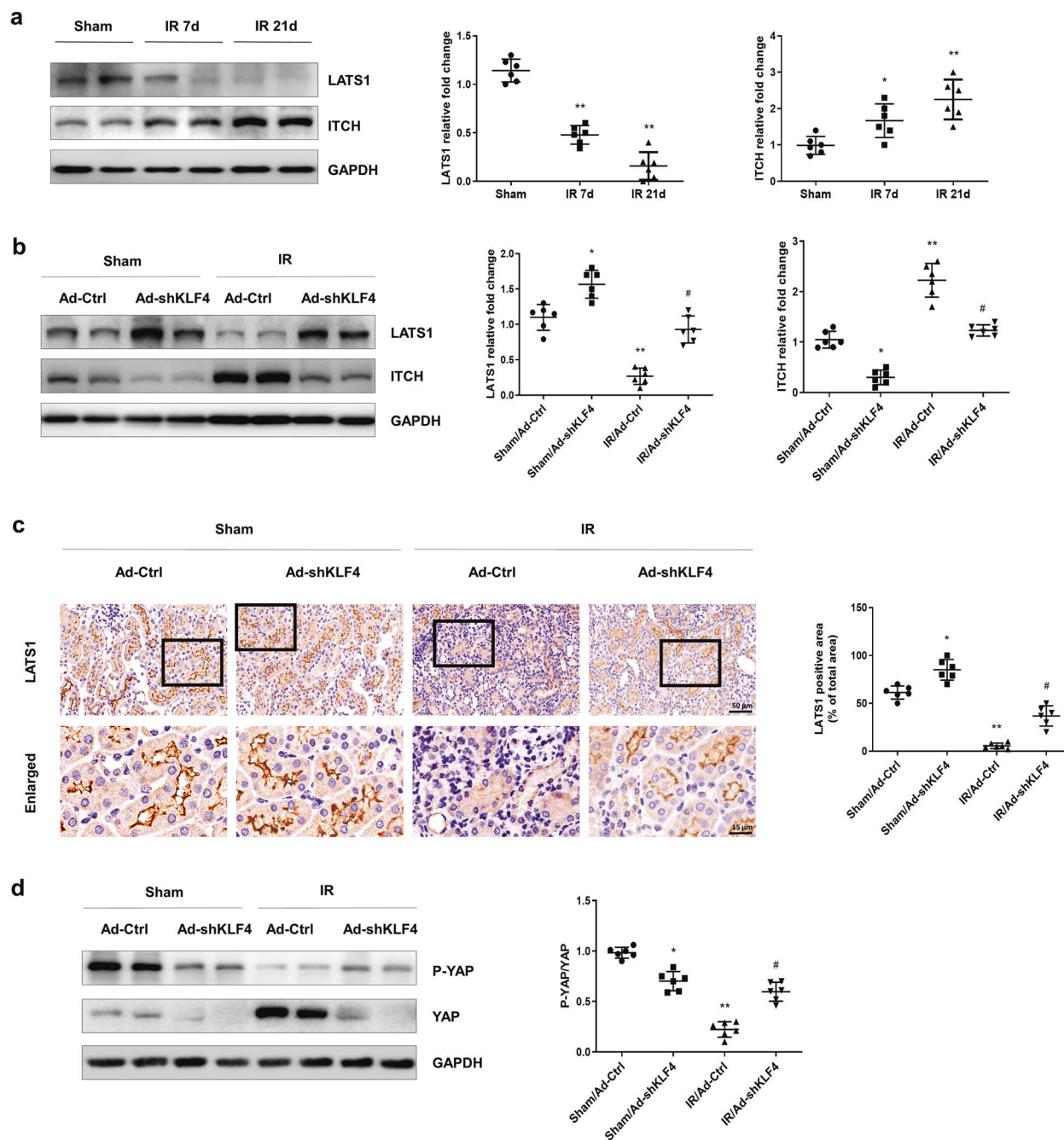
Sustained activation of KLF4-YAP promotes renal fibrosis
D Xu et al.

448

Fig. 8 KLF4 is critical for YAP activation after IR induction. a Western blotting was conducted to determine the protein levels of ITCH and LATS1 on the 7th and 21st days after IR induction. Six mice per group. Data are presented as the means ± SEM. *$P < 0.05$, **$P < 0.01$ versus the sham group. **b** The expression of ITCH and LATS1 in the four groups was assessed by Western blotting as indicated. **c** IHC was performed to visualize the distribution of LATS1. Boxed areas are enlarged and presented in the figures below. **d** Expression of P-YAP and YAP in four groups was assessed by Western blotting as indicated. The ratio of P-YAP/YAP was analyzed. $n = 6$ mice in each group. Data are presented as the means ± SEM. *$P < 0.05$, **$P < 0.01$ versus the sham/Ad-Ctrl group. #$P < 0.05$ versus the IR/Ad-Ctrl group, IR ischemia-reperfusion.

of TGF-β and CTGF in renal tubular epithelial cells and then stimulates the activation of interstitial fibroblasts and promotes fibrosis. KLF4, a reprogramming factor, is implicated in renal fibrosis because it stimulates the expression and activation of YAP. KLF4 increases the expression of YAP directly and facilitates YAP activation by increasing the expression of ITCH. The observation that YAP nuclear translocation was increased in the biopsy samples from CKD patients strengthens the clinical relevance of the study. Therefore, we propose that accurately terminating the activation of the Hippo pathway might be beneficial to the kidney after AKI. However, the reason for the sustained increase in the reprogramming factor remains to be elucidated.

In conclusion, sustained activation of YAP in the post-acute phase of AKI is implicated in the chronic decline of renal function and development of interstitial fibrosis. The reprogramming factor KLF4 is critical for the sustained high expression and activation of YAP.
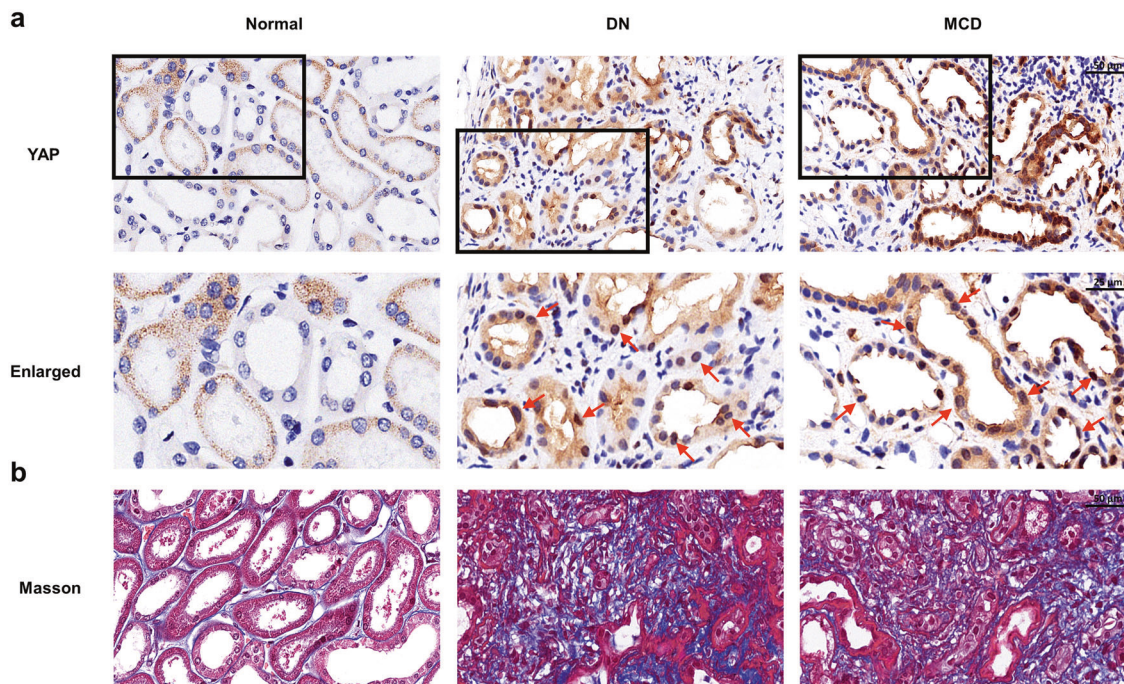
Sustained activation of KLF4-YAP promotes renal fibrosis
D Xu et al.

449

Fig. 9 Elevated YAP is associated with renal fibrosis in clinical nephropathy. a Representative images show the localization and expression of YAP in various types of human chronic kidney disease (CKD). Normal controls were obtained from the unaffected parts of nephrectomy specimens obtained from renal carcinoma patients. Boxed areas are enlarged and presented in the figures below. Red arrows indicate YAP-positive tubules. **b** Human kidney sections were subjected to Masson's staining. DN diabetic nephropathy, MCD minimal change disease.

AUTHOR CONTRIBUTIONS
DX, LML, and WZ participated in the design of the study. DX wrote the paper. DX and PPC were involved in performing the experiments and analyzing the results. DX, PPC, PQZ, FY, QC, ZLZ, HYX, JYL, JYN, YZW, SJC, LZ, XXW, and JL took part in the revision of the manuscript.

ADDITIONAL INFORMATION
The online version of this article (https://doi.org/10.1038/s41401-020-0463-x) contains supplementary material, which is available to authorized users.

REFERENCES
1. Vanmassenhove J, Van Biesen W, Vanholder R, Lameire N. Subclinical AKI: ready for primetime in clinical practice? J Nephrol. 2019;32:9–16.
2. Parikh CR, Mansour SG. Perspective on clinical application of biomarkers in AKI. J Am Soc Nephrol. 2017;28:1677–85.
3. See EJ, Jayasinghe K, Glassford N, Bailey M, Johnson DW, Polkinghorne KR, et al. Long-term risk of adverse outcomes after acute kidney injury: a systematic review and meta-analysis of cohort studies using consensus definitions of exposure. Kidney Int. 2019;95:160–72.
4. Coca SG, Singanamala S, Parikh CR. Chronic kidney disease after acute kidney injury: a systematic review and meta-analysis. Kidney Int. 2012;81:442–8.
5. Xu D, Wang B, Chen P, Wang YZ, Miao NJ, Yin F, et al. c-Myc promotes tubular cell apoptosis in ischemia-reperfusion-induced renal injury by negatively regulating c-FLIP and enhancing FasL/Fas-mediated apoptosis pathway. Acta Pharmacol Sin. 2019;40:1058–66.
6. Srisawat N, Murugan R, Kellum JA. Repair or progression after AKI: a role for biomarkers? Nephron Clin Pr. 2014;127:185–89.
7. Ferenbach DA, Bonventre JV. Mechanisms of maladaptive repair after AKI leading to accelerated kidney ageing and CKD. Nat Rev Nephrol. 2015;11:264–76.
8. Chatauret N, Badet L, Barrou B, Hauet T. Ischemia-reperfusion: from cell biology to acute kidney injury. Prog Urol. 2014;24(Suppl 1):S4–12.
9. Bonventre JV. Primary proximal tubule injury leads to epithelial cell cycle arrest, fibrosis, vascular rarefaction, and glomerulosclerosis. Kidney Int Suppl (2011). 2014;4:39–44.
10. Tanaka S, Tanaka T, Nangaku M. Hypoxia as a key player in the AKI-to-CKD transition. Am J Physiol Ren Physiol. 2014;307:F1187–95.
11. Bonventre JV. Maladaptive proximal tubule repair: cell cycle arrest. Nephron Clin Pract. 2014;127:61–4.
12. Goldstein SL, Jaber BL, Faubel S, Chawla LS. AKI transition of care: a potential opportunity to detect and prevent CKD. Clin J Am Soc Nephrol. 2013;8:476–83.
13. Basile DP, Bonventre JV, Mehta R, Nangaku M, Unwin R, Rosner MH, et al. Progression after AKI: understanding maladaptive repair processes to predict and identify therapeutic treatments. J Am Soc Nephrol. 2016;27:687–97.
14. Humphreys BD, Cantaluppi V, Portilla D, Singbartl K, Yang L, Rosner MH, et al. Targeting endogenous repair pathways after AKI. J Am Soc Nephrol. 2016;27:990–8.
15. Maas K, Mirabal S, Penzias A, Sweetnam PM, Eggan KC, Sakkas D. Hippo signaling in the ovary and polycystic ovarian syndrome. J Assist Reprod Genet. 2018;35:1763–71.
16. Frum T, Murphy TM, Ralston A. HIPPO signaling resolves embryonic cell fate conflicts during establishment of pluripotency in vivo. Elife. 2018;7:e42298. https://doi.org/10.7554/eLife.42298.
17. 5Volckaert T, Yuan T, Yuan J, Boateng E, Hopkins S, Zhang JS, et al. Hippo signaling promotes lung epithelial lineage commitment by curbing Fgf10 and beta-catenin signaling. Development. 2019;146:dev166454. https://doi.org/10.1242/dev.166454.
18. Nair PR, Wirtz D. Enabling migration by moderation: YAP/TAZ are essential for persistent migration. J Cell Biol. 2019;218:1092–3.
19. Han H, Yang B, Nakaoka HJ, Yang J, Zhao Y, Le Nguyen K, et al. Hippo signaling dysfunction induces cancer cell addiction to YAP. Oncogene. 2018;37:6414–24.
20. Lian I, Kim J, Okazawa H, Zhao J, Zhao B, Yu J, et al. The role of YAP transcription coactivator in regulating stem cell self-renewal and differentiation. Genes Dev. 2010;24:1106–18.
21. White SM, Murakami S, Yi C. The complex entanglement of Hippo-Yap/Taz signaling in tumor immunity. Oncogene. 2019;38:2899–909.
22. Sugihara T, Isomoto H, Gores G, Smoot R. YAP and the hippo pathway in cholangiocarcinoma. J Gastroenterol. 2019;54:485–91.

23. Chen J, You H, Li Y, Xu Y, He Q, Harris RC. EGF receptor-dependent YAP activation is important for renal recovery from AKI. J Am Soc Nephrol. 2018;29:2372–85.

24. Sharma M, Radhakrishnan R. CTGF is obligatory for TGF-beta1 mediated fibrosis in OSMF. Oral Oncol. 2016;56:e10–11.

25. Li L, Dong L, Wang Y, Zhang X, Yan J. Lats1/2-mediated alteration of hippo signaling pathway regulates the fate of bone marrow-derived mesenchymal stem cells. Biomed Res Int. 2018;2018:4387932.

26. Nishioka N, Inoue K, Adachi K, Kiyonari H, Ota M, Ralston A, et al. The hippo signaling pathway components Lats and Yap pattern Tead4 activity to distinguish mouse trophectoderm from inner cell mass. Dev Cell. 2009;16:398–410.

27. Ho KC, Zhou Z, She YM, Chun A, Cyr TD, Yang X. Itch E3 ubiquitin ligase regulates large tumor suppressor 1 stability. Proc Natl Acad Sci USA. 2011;108:4870–5.

28. Marzi I, Cipolleschi MG, D'Amico M, Stivarou T, Rovida E, Vinci MC, et al. The involvement of a Nanog, Klf4 and c-Myc transcriptional circuitry in the intertwining between neoplastic progression and reprogramming. Cell Cycle. 2013;12:353–64.

29. Choi H, Roh J. Role of klf4 in the regulation of apoptosis and cell cycle in rat granulosa cells during the periovulatory period. Int J Mol Sci. 2018;20:87. https://doi.org/10.3390/ijms20010087.

30. Tang J, Zhong G, Wu J, Chen H, Jia Y. SOX2 recruits KLF4 to regulate nasopharyngeal carcinoma proliferation via PI3K/AKT signaling. Oncogenesis. 2018;7:61. https://doi.org/10.1038/s41389-018-0074-2.

31. Cheng Z, Zou X, Jin Y, Gao S, Lv J, Li B, et al. The role of KLF4 in Alzheimer's disease. Front Cell Neurosci. 2018;12:325. https://doi.org/10.3389/fncel.2018.00325.

32. Brauer PR, Kim JH, Ochoa HJ, Stratton ER, Black KM, Rosencrans W, et al. Kruppel-like factor 4 mediates cellular migration and invasion by altering RhoA activity. Cell Commun Adhes. 2018;24:1–10.

33. Qi XT, Li YL, Zhang YQ, Xu T, Lu B, Fang L, et al. KLF4 functions as an oncogene in promoting cancer stem cell-like characteristics in osteosarcoma cells. Acta Pharmacol Sin. 2019;40:546–55.

34. Shen Y, Miao N, Wang B, Xu J, Gan X, Xu D, et al. c-Myc promotes renal fibrosis by inducing integrin alphav-mediated transforming growth factor-beta signaling. Kidney Int. 2017;92:888–99.

35. Pan Y, Alegot H, Rauskolb C, Irvine KD. The dynamics of Hippo signaling during Drosophila wing development. Development. 2018;145:dev165712. https://doi.org/10.1242/dev.165712.

36. Xu D, Chen P, Wang B, Wang Y, Miao N, Yin F, et al. NIX-mediated mitophagy protects against proteinuria-induced tubular cell apoptosis and renal injury. Am J Physiol Renal Physiol. 2019;316:F382–95.

37. Bernhardt A, Fehr A, Brandt S, Jerchel S, Ballhause TM, Philipsen L, et al. Inflammatory cell infiltration and resolution of kidney inflammation is orchestrated by the cold-shock protein Y-box binding protein-1. Kidney Int. 2017;92:1157–77.

38. Fu Y, Tang C, Cai J, Chen G, Zhang D, Dong Z. Rodent models of AKI-CKD transition. Am J Physiol-Ren. 2018;315:F1098–106.

39. Luo C, Zhou S, Zhou Z, Liu Y, Yang L, Liu J, et al. Wnt9a promotes renal fibrosis by accelerating cellular senescence in tubular epithelial cells. J Am Soc Nephrol. 2018;29:1238–56.

40. Liu BC, Tang TT, Lv LL, Lan HY. Renal tubule injury: a driving force toward chronic kidney disease. Kidney Int. 2018;93:568–79.

41. Tan RJ, Zhou D, Liu Y. Signaling crosstalk between tubular epithelial cells and interstitial fibroblasts after kidney injury. Kidney Dis. 2016;2:136–44.

42. Szeto SG, Narimatsu M, Lu M, He X, Sidiqi AM, Tolosa MF, et al. YAP/TAZ are mechanoregulators of TGF-beta-Smad signaling and renal fibrogenesis. ed. 2016;3117–28.

43. Liu Y. Cellular and molecular mechanisms of renal fibrosis. Nat Rev Nephrol. 2011;7:684–96.

44. Macconi D, Remuzzi G, Benigni A. Key fibrogenic mediators: old players. Renin-angiotensin system. Kidney Int Suppl (2011). 2014;4:58–64.

45. Ito Y, Aten J, Bende RJ, Oemar BS, Rabelink TJ, Weening JJ, et al. Expression of connective tissue growth factor in human renal fibrosis. Kidney Int. 1998;53:853–61.

46. Wolf G. Renal injury due to renin-angiotensin-aldosterone system activation of the transforming growth factor-beta pathway. Kidney Int. 2006;70:1914–9.

47. Zhou D, Li Y, Zhou L, Tan RJ, Xiao L, Liang M, et al. Sonic hedgehog is a novel tubule-derived growth factor for interstitial fibroblasts after kidney injury. J Am Soc Nephrol. 2014;25:2187–200.

48. Ding H, Zhou D, Hao S, Zhou L, He W, Nie J, et al. Sonic hedgehog signaling mediates epithelial-mesenchymal communication and promotes renal fibrosis. J Am Soc Nephrol. 2012;23:801–13.

49. Yoshida T, Yamashita M, Iwai M, Hayashi M. Endothelial Kruppel-Like factor 4 mediates the protective effect of statins against ischemic AKI. J Am Soc Nephrol. 2016;27:1379–88.